Science of the Total Environment 856 (2023) 158937

Contents lists available at ScienceDirect

Science of the Total Environment

journal homepage: www.elsevier.com/locate/scitotenv

Mercury in a birch forest in SW Europe: Deposition flux by litterfall and pools in aboveground tree biomass and soils

Melissa Méndez-López [a,b,*], Andrea Parente-Sendín [a,b], Noemi Calvo-Portela [a,b], Antía Gómez-Armesto [a,b], Cristina Eimil-Fraga [c], Flora Alonso-Vega [a,b], Manuel Arias-Estévez [a,b], Juan Carlos Nóvoa-Muñoz [a,b]

[a] Universidade de Vigo, Departamento de Bioloxía Vexetal e Ciencia do Solo, Área de Edafoloxía e Química Agrícola, Facultade de Ciencias, As Lagoas s/n, 32004 Ourense, Spain
[b] Campus da Auga, Universidade de Vigo, Laboratorio de Tecnoloxía e Diagnose Ambiental, Rúa Canella da Costa da Vela 12, 32004 Ourense, Spain
[c] Unidad de Gestión Ambiental y Forestal Sostenible, Escuela Politécnica Superior de Ingeniería, Universidade de Santiago de Compostela, Rúa Benigno Ledo s/n, 27002 Lugo, Spain

HIGHLIGHTS

- Birch leaves are the major contributor to Hg deposition flux by litterfall.
- Woody tissues represent the largest Hg reservoir in the aboveground birch biomass.
- The soil highest Hg concentrations were found in the organic horizons.
- The mineral soil is the major pool of Hg, exempt from environmental disturbances.

GRAPHICAL ABSTRACT

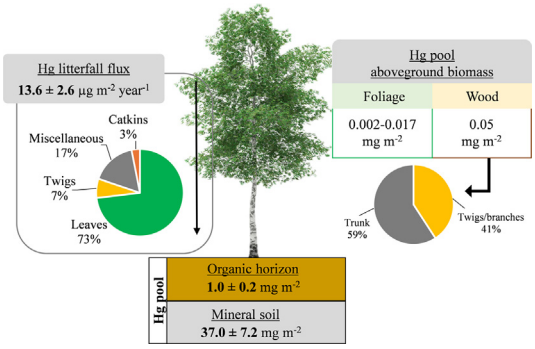

ARTICLE INFO

Editor: Manuel Esteban Lucas-Borja

Keywords:
Heavy metal
Pool
Birch
Betula alba
Climate
Growing season

ABSTRACT

Atmospheric mercury (Hg) is largely assimilated by vegetation and subsequently transferred to the soil by litterfall, which highlights the role of forests as one of the largest global Hg sinks within terrestrial ecosystems. We assessed the pool of Hg in the aboveground biomass (leaves, wood, bark, branches and twigs), the Hg deposition flux through litterfall over two years (by sorting fallen biomass in leaves, twigs, reproductive structures and miscellaneous) and its accumulation in the soil profile in a deciduous forest dominated by *Betula alba* from SW Europe. The total Hg pool in the aboveground birch biomass was in the range 532–683 mg ha^{-1}, showing the following distribution by plant tissues: well-developed leaves (171 mg ha^{-1}) > twigs (160 mg ha^{-1}) > bark (159 mg ha^{-1}) > bole wood (145 mg ha^{-1}) > fine branches (25 mg ha^{-1}) > thick branches (24 mg ha^{-1}) > newly sprouted leaves (20 mg ha^{-1}). The total Hg deposition fluxes through litterfall were 15.4 and 11.7 μg m^{-2} yr^{-1} for the two years studied, with the greatest contribution coming from birch leaves (73 %). In the soil profile, the pool of Hg in the mineral soil (37.0 mg m^{-2}) was an order of magnitude higher than in the organic horizons (1.0 mg m^{-2}), mostly conditioned by parameters such as soil bulk density and thickness, total C and N contents and the presence of certain Al compounds.

1. Introduction

Mercury is a heavy metal of global concern that is transported over long distances through the atmosphere until deposited over aquatic and terrestrial ecosystems (Ma et al., 2015). Atmospheric Hg can derive either from

* Corresponding author at: Universidade de Vigo, Departamento de Bioloxía Vexetal e Ciencia do Solo, Área de Edafoloxía e Química Agrícola, Facultade de Ciencias, As Lagoas s/n, 32004 Ourense, Spain.
E-mail address: memendez@uvigo.es (M. Méndez-López).

http://dx.doi.org/10.1016/j.scitotenv.2022.158937
Received 4 July 2022; Received in revised form 15 September 2022; Accepted 18 September 2022
Available online 24 September 2022

the Earth's crust or from anthropic activities (Driscoll et al., 2013). The major chemical forms of mercury found in the atmosphere are gaseous elemental mercury (GEM), reactive gaseous mercury (RGM) and particulate-bound mercury (PBM) (Driscoll et al., 2013). Atmospheric mercury can reach terrestrial ecosystems through the wet deposition of RGM and PBM or via dry deposition of GEM. Wet deposition of Hg occurs rapidly but occasionally, while dry deposition is slower but permanent in time, thus making the latter the most important Hg deposition pathway in many ecosystems (Munthe et al., 2004; Graydon et al., 2008; Obrist et al., 2021).

In forested areas, vegetation plays a key role as a sink for atmospheric Hg (Agnan et al., 2016; Zhu et al., 2016). RGM and PBM adsorb to leaf surface (Rea et al., 2001) and GEM penetrates leaf cuticles through stomata and non-stomatal pathways (Rutter et al., 2011). In addition, some PBM could remain bound to the leaf surface after rainfall events, contributing to some extent to the total Hg content in foliar tissues. Over 80 % of mercury accumulated in foliage deposits to the soil surface through the fall of senescent plant biomass, via litterfall (Jiskra et al., 2015; Wang et al., 2016), although Hg can also be transferred to soils by leaf surface wash off, via throughfall (Wright et al., 2016).

Although there is a considerable knowledge about the role of litterfall in the deposition of Hg to forest soils, most of the studies carried out to date were focused on forests from North America and Asia (Wright et al., 2016). In Europe, studies on Hg deposition through litterfall or on Hg storage in aboveground biomass are scarce, being mainly performed in northern and central European forests in areas characterized by continental and subpolar humid climates (Munthe et al., 1995; Larssen et al., 2008; Jiskra et al., 2015; Navrátil et al., 2016, 2019). For deciduous species, these climatic conditions shorten the foliar growth period reducing the amount of Hg sequestered by leaves and decreasing the flux of Hg through litterfall. Furthermore, most of the studies carried out in Europe lack information about the seasonal variation of Hg deposition by litterfall as well as the contribution of different aboveground plant tissues. Although leaves are a major component of litterfall (Sun et al., 2021), the aboveground biomass offers other plant tissues which can store Hg for longer periods (bark, branches, twigs and bole wood), contributing somewhat to the medium and long-term Hg deposition on topsoil (Friedli et al., 2007; Gómez-Armesto et al., 2020b; Navrátil et al., 2019; Obrist et al., 2012).

Soils are considered the main Hg reservoir in forest ecosystems (Grigal, 2003; Obrist et al., 2018), but this ability can vary according to the climatic characteristics of the study area. Thus, a decrease in topsoil Hg pools has been observed from the northern to the southern latitudes of the northern Hemisphere (Ballabio et al., 2021) due to changes in the vegetation type, which are closely associated with climatic characteristics (Wang et al., 2019). Moreover, Hg uptake by vegetation was demonstrated to be higher during the summer growing season, when warmer temperatures make vegetation more active for gas exchange with the atmosphere (Jiskra et al., 2018). Furthermore, despite the expected higher Hg re-emission at lower latitudes, warmer temperatures enable an earlier start and a later end of the vegetation growing season (Wu et al., 2021), favouring the removal of atmospheric Hg by plant uptake for a longer period. Consequently, higher Hg storage in aboveground biomass and Hg deposition fluxes through litterfall could be expected.

New insights into the fate of Hg in the soil-plant system in temperate deciduous forests are needed to better understand how it can be modified under current scenarios of changing environmental conditions driven by human activities. This is of particular interest in southern and western areas of Atlantic Europe, which are very sensitive to the impacts of global warming and land use changes, and because studies on the biogeochemical dynamics of Hg in terrestrial ecosystems are almost absent in this part of Europe. Furthermore, to our knowledge, there are no studies focused on the behavior of birch species in Hg accumulation and its transfer to the upper soil layers through litterfall, despite being a widespread genus in European areas characterized by cold and moist climates (Beck et al., 2016).

Following this background, the study aims to improve the knowledge on the terrestrial Hg cycle in a deciduous birch forest by monitoring Hg deposition through litterfall over two growing seasons, estimating the amount of Hg stored in the aboveground birch biomass and assessing the amount of Hg accumulated in the soils located under the forest. Climatic parameters, such as temperature and precipitation, will be considered as potential factors influencing Hg deposition, while the physico-chemical soil properties will be assessed to explain the accumulation of Hg in the soil. The results are expected to contribute to extend the knowledge of the role of deciduous species in the Hg cycle in temperate forest ecosystems, especially in the case of species belonging to the genus *Betula*, that cover a wide area along the European Atlantic coast and northern and central Europe (EUFORGEN, 2016).

2. Material and methods

2.1. Study area description

The study area is located in the NW of the Iberian Peninsula (geographic coordinates: 42°13′46.4"N - 8°20′17.5"W) (Fig. S1), which is characterized by an Atlantic climate with a strong oceanic influence leading to wet winters and warm summers (Martínez Cortizas and Pérez Alberti, 1999). The meteorological data from 2019 to 2021 results in mean annual temperatures of 13.5 °C and total annual rainfall up to 1600 mm. The study plot is located at 700 m above sea level and lies on a lithological substrate composed of granitic rocks. The forest vegetation that covers the study plot is representative of the Atlantic deciduous forests often found in western Europe, which consists of a secondary succession mostly dominated by birch (*Betula alba*, L.), accompanied by some individuals of *Quercus robur* (L.), *Salix atrocinerea* (Brot.) and *Pinus pinaster* (Aiton) as remains of an old plantation in the study area. The stand, with an area of 4500 m^2, was established in the middle of a dense birch forest mass, being surrounded by two small streams. There are no significant point sources of mercury emission close (< 60 km) to the study area.

2.2. Litterfall and plant tissues sampling

Litterfall was collected from 10 conical collectors made of nylon net with a circular opening of 0.24 m^2, which were randomly distributed throughout the study plot given its high cover degree (> 90 %; Table 1), avoiding surrounding individuals of other species. Additional information about litterfall collectors is detailed in Text S1 and Fig. S2. Litterfall collected in each trap was stored individually in correctly identified zip bags. Once in the laboratory, samples were dried in a forced-air oven at 35 °C for at least a week. Dried samples were separated into the following four fractions: birch leaves, twigs, reproductive structures and miscellaneous, i.e., remaining plant material composed of leaves of other tree species, bark, lichens, moss and unidentifiable plant debris.

In order to assess Hg storage in aboveground biomass, three subplots of 225 m^2 (15 × 15 m) were established within the original study plot at the beginning of the growing season in March 2021. We selected the beginning of the growing season for aboveground biomass sampling to obtain an estimate of the lower end of its Hg pool, as well as to facilitate the sampling of newly sprouted birch leaves to serve as a baseline for the calculation of the Hg accumulation rate in foliar biomass throughout the growing season. In each subplot, three representative birch trees (healthy and with a large crown) were selected and a well-developed branch from the upper third

Table 1
Mean values and (±) standard deviation, minimum and maximum values of several forestry characteristics for the studied plot (n = 3 subplots).

Parameter	$\bar{x}$ ± sd	Min.	Max.
Density (trees ha^{-1})	2015 ± 257	1867	2311
Basal area (m^2 ha^{-1})	26.9 ± 4.1	22.8	31.0
Dominant height (m)	16.3 ± 0.5	15.8	16.8
Mean height (m)	13.8 ± 0.7	13.0	14.2
Mean diameter (cm)	12.2 ± 1.6	10.3	13.4
Canopy cover (%)	> 90	–	–

of the crown of each tree was cut off. From each branch, samples from the following plant tissues were collected: newly sprouted birch leaves, thick branches (Ø > 2 cm), fine branches (Ø = 0.5–2 cm) and twigs (Ø < 0.5 cm). The bark of fine and thick branches was removed, leaving only the woody tissue in order to avoid interference between the bark and the wood in the subsequent Hg analysis (it was not possible to perform this separation on the twigs due to their thinness). Composite samples of bark and bole wood were also taken from the three birch trees of each subplot. The total height and diameter at breast height of all the birch trees included in the subplots were measured (Table 1). These data were used to calculate the total aboveground biomass of each plant tissue per unit area, by applying the allometric equations described for birch in NW Spain by Gómez-García et al. (2013) (Text S3).

Before Hg analysis, samples from litterfall and aboveground biomass were ground to a particle size <0.5 mm and subsequently milled with a mechanical agate mortar to increase sample homogeneity by further reducing particle size. The grinder and mill were properly cleaned between different samples with diluted HCl and distilled water to avoid cross-contamination. Handling of aboveground biomass and litterfall samples during fieldwork and in the laboratory was done with disposable gloves.

The percentage of humidity was estimated by drying an aliquot of ground sample in an oven at 105 °C. This humidity percentage was used to correct total Hg concentrations on a constant dry weight basis.

2.3. Soil sampling and physico-chemical analysis

Samples of organic horizons were taken at four randomly selected points of the study plot, differentiating the Oi from the Oe + Oa subhorizons. Organic soil samples were taken on a surface of 50 × 50 cm, writing down the thickness of each subhorizon and transferring the entire soil mass into plastic bags.

The mineral soil samples were collected in two of the points where the organic horizons were sampled. For this purpose, a square hole was dug, taking samples at 5 cm intervals up to 20 cm, and thereafter, at 10 cm intervals up to a depth of 60 cm. In order to determine the mineral soil bulk density, soil cores were taken at the same intervals using stainless steel cylinders of 100 cm^3. In addition, samples of fresh soil parent material were taken in the study stand. All soil samples were transported to the laboratory on the same day of sampling. Both soils were classified tentatively as Haplic Umbrisol (Alumic, Arenic) (IUSS Working Group WRB, 2015).

Once in the laboratory, large pieces of wood and branches were removed from the organic horizons as well as stones and gravel in the case of mineral soil layers. Afterward, the organic and mineral soil samples were air-dried in an oven at 35 °C for 10 days. The calculation of the bulk density of the organic horizons was based on the dry weight and thickness of each organic layer and the area where they were collected (0.25 m^2). For mineral layers, the soil taken in the stainless steel cylinders was oven-dried to constant weight at 105 °C for two days and weighed to calculate their bulk density. The processing of the soil samples started with grinding the organic horizons to 4 mm and sieving the mineral horizons to 2 mm. Samples of parent material were cleaned with distilled water to remove dust and soil remains, then dried and crushed to smaller particles. Finally, an aliquot of each ground organic horizon, sieved mineral horizon and crushed rocks was finely powdered in a mechanical agate mortar.

The soil general characterization included a texture analysis as a physical characteristic and the determination of pH in water, total C and N and the distribution of Fe and Al as chemical characteristics. Details of the procedures for soil characterization are described in Text S2 (Supplementary material).

2.4. Mercury analysis in vegetation and soil samples

Total Hg concentration (*THg*) was analyzed in ground samples of litterfall, aboveground biomass, organic and mineral soil and parent material. For *THg* measurement, a Milestone tri-cell Direct Mercury Analyzer (DMA-80) was used, following the US EPA method 7473 based on sample thermal decomposition, amalgamation, and atomic absorption spectrometry. Each sample was analyzed in duplicate ensuring that the coefficient of variation (CV) did not exceed 10 %. Otherwise, the analysis would be repeated until a suitable CV was obtained. Approximately 100 mg of each individual sample were weighed in nickel vessels for total Hg analysis.

For quality assurance and control (QA/QC), the following standard reference materials were measured at the beginning of the analysis and every twelve samples: NIST 1547 (peach leaves; 31 ± 7 μg Hg kg^{-1}), NIST 1570a (spinach leaves; 30 ± 2 μg Hg kg^{-1}) and BCR 142 R (sandy soil, 67 ± 11 μg Hg kg^{-1}), obtaining recovery rates of 100.1 ± 5.8, 85.1 ± 2.4 and 101.2 ± 2.7 %, respectively.

2.5. Calculation of litterfall and Hg fluxes and Hg pools in plant tissues and soil

Litterfall and mercury fluxes were calculated for each fraction (leaves, twigs, reproductive structures and miscellaneous) and collector. Thus, the litterfall flux (g m^{-2}) of a specific fraction (LF_i) was calculated following the Eq. (1):

$$LF_i = \frac{W_i}{A_C} \quad (1)$$

where W_i (grams) is the amount of biomass (corrected on a constant dry weight basis) of a specific fraction (i) that was picked up from a collector whose area is A_C (m^2).

Moreover, mercury deposition flux (ng m^{-2}) for a given litterfall fraction (HgF_i) was calculated by applying the Eq. (2):

$$HgF_i = LF_i \; x \; THg_i \quad (2)$$

where LF_i and THg_i represent the litterfall flux (g m^{-2}) and total Hg concentration (ng g^{-1}) of a specific litterfall fraction (i), respectively.

Mean monthly fluxes of litterfall and Hg for each fraction were calculated as the average of the fluxes obtained for all the collectors of the stand (n = 10). The annual litterfall and Hg fluxes of a specific fraction were calculated as the sum of its monthly averages (n = 12), considering two annual periods: from May 2019 to April 2020 and from May 2020 to April 2021. The monthly total litterfall flux (*TLF*) was the sum of the mean fluxes of leaves, twigs, reproductive structures and miscellaneous obtained in a given month. The annual total litterfall flux was the sum of the twelve monthly *TLF* defining each of the two periods evaluated. The estimation of total Hg flux through the whole litterfall (*THgF*) on a monthly and annual basis was done as previously described for total litterfall fluxes (*TLF*).

The Hg pool in the aboveground biomass of the analyzed plant tissues, including newly sprouted leaves, branches, twigs, bark and bole wood, was denoted as *THgW* and expressed in mg ha^{-1}. Values of *THgW* were obtained by multiplying the total biomass of each plant tissue (estimated according to the allometric equations previously cited) by its corresponding Hg concentration. In this calculation, the surface of each of the three subplots (225 m^2) was taken into account for the conversion of Hg pools in aboveground biomass to an area scale.

The pool of Hg in soil (*PHg*), in μg m^{-2}, was calculated for each organic and mineral layer considering their individual Hg concentration, bulk density and thickness, similarly to Zhou et al. (2017).

2.6. Statistical treatment

Statistical analyses were carried out using the 25th version of IBM SPSS Statistics software for Windows. The influence of litterfall fraction (leaves, twigs, reproductive structures and miscellaneous), plant tissue (newly sprouted leaves, thick branches, fine branches, twigs, bole wood and bark) and time (months) on Hg concentration and its deposition fluxes was checked by applying suitable non-parametric statistical tests such as Kruskal-Wallis (H), Wilcoxon (Z) and Mann-Whitney (U). In addition, a Spearman rank correlation (ρ) was performed to establish relationships

between the parameters obtained from litterfall (i.e. *THg* concentration and biomass and Hg fluxes) and soil samples (bulk density, organic matter, Al and Fe compounds) and climatic characteristics (temperature and precipitation). Statistical significance was considered when $p < 0.05$ unless otherwise noted.

3. Results

3.1. Litterfall fluxes

The annual total litterfall flux (*TLF*) was 537 g m^{-2} yr^{-1} with somewhat greater values in the 2019–2020 period (603 g m^{-2} yr^{-1}) than in 2020–2021 (470 g m^{-2} yr^{-1}). The fraction that contributed the most to the annual *TLF* was birch leaves, representing 63 and 68 % in 2019–2020 (348 g m^{-2} yr^{-1}) and 2020–2021 (318 g m^{-2} yr^{-1}), respectively. The contribution of other fractions (twigs, miscellaneous and reproductive structures) to the annual *TLF* varied between 9 and 15 % in the 2019–2020 period and between 3 and 22 % in 2020–2021 (Table S1). A Kruskal-Wallis test revealed that the fraction of senescent biomass was a significant variance factor for annual *TLF* in 2019–2020 ($H = 86.214$; $p < 0.01$; $n = 428$) and 2020–2021 ($H = 87.527$; $p < 0.01$; $n = 410$).

The monthly total litterfall fluxes (*TFL*) peaked in September and October 2019 (136 g m^{-2}) and in July (122 g m^{-2}) and September 2020 (119 g m^{-2}), whereas the lowest values (<12 g m^{-2}) were found in winter (January and February). Consistent with the previously detailed annual trend, the highest monthly fluxes were observed in birch leaves, which showed their highest contribution between July and October of both periods (2019–2020 and 2020–2021) with values ranging from 15 to 133 g m^{-2} (Table S1). Almost 90 % of the total annual leaf fall is concentrated during that period. The monthly fluxes of twigs were highly variable throughout both periods (range 0–18 g m^{-2}; Table S1), showing maximum values during the winter months. The flux of miscellaneous also experienced a large monthly variation (range from 0.2 to 21.5 g m^{-2}) but without a clear trend throughout the year. Finally, the deposition of reproductive structures was concentrated in March and April with fluxes reaching 37.3 g m^{-2}, contributing up to 58 % of the total litterfall flux during such months. In both studied periods, the monthly *TLF* were significantly different depending on the month ($H = 114.198$; $p < 0.01$; $n = 428$ and $H = 100.968$; $p < 0.01$; $n = 410$ for 2019–2020 and 2020–2021, respectively).

3.2. Mercury concentration in litterfall fractions

The mean total Hg concentration (*THg*) in the fractions composing the litterfall are shown for every month in Table S2. The levels of *THg* followed the sequence: miscellaneous (44 and 32 μg kg^{-1}) > birch leaves (23 and 29 μg kg^{-1}) > twigs (20 and 17 μg kg^{-1}) > reproductive structures (7 and 11 μg kg^{-1}). The values of *THg* were significantly different among fractions in both the 2019–2020 ($H = 246.378$; $p < 0.01$; $n = 428$) and the 2020–2021 ($H = 147.809$; $p < 0.01$; $n = 410$) periods.

On a monthly basis, *THg* in birch leaves showed the lowest mean values in March (3–11 μg kg^{-1}) whereas the highest values were found in January (64 μg kg^{-1}). Total Hg in birch leaves increased steadily, from leaf sprouting in early spring until its withering and consequent drop and fall in early autumn (September–October). The month was a significant influencing factor on *THg* of birch leaves in 2019–2020 ($H = 84.632$; $p < 0.01$; $n = 89$) and 2020–2021 ($H = 101.460$; $p < 0.01$; $n = 104$). The Hg accumulation rate in birch leaves, estimated as the slope of the linear regression fit of their *THg* concentrations during the growing season (from March to September), was 0.18 μg kg^{-1} day^{-1} (Fig. 1).

Regarding the fraction composed of miscellaneous, the peaks of *THg* occurred in June 2019 and January and November 2020 with values over 70 μg kg^{-1} (Table S2). The monthly variation of *THg* in twigs showed a range from 7 μg kg^{-1} (February 2020) to 29 μg kg^{-1} (May 2019), without a clear trend over the studied periods (Table S2). Total Hg in reproductive structures also did not show a clear trend throughout the year in both studied periods, with mean monthly values ranging from 2 to 20 μg kg^{-1} (Table S2).

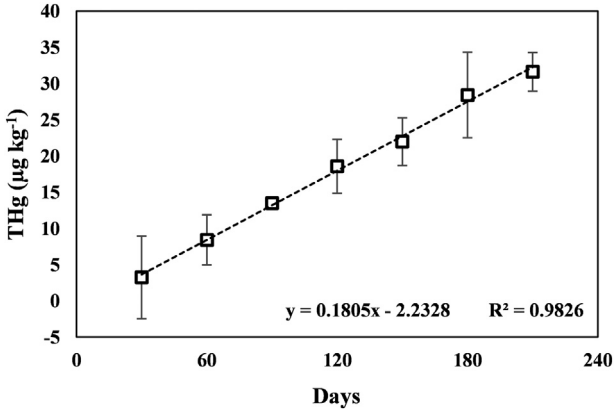

Fig. 1. Evolution of THg in birch leaves over the course of the growing season (from March to September), based on the monthly average of the two studied periods. The error bars represent the standard deviation.

Similar to birch leaves, *THg* concentrations in twigs, miscellaneous and reproductive structures varied significantly ($p < 0.01$) depending on the month (Table S3).

3.3. Mercury deposition fluxes through litterfall

The annual Hg fluxes through litterfall (*THgF*), taking into account the contribution of leaves, miscellaneous, twigs and reproductive structures, were 15.4 and 11.7 μg m^{-2} yr^{-1} for the 2019–2020 and 2020–2021 periods, respectively. A Wilcoxon test performed with monthly *THgF* values resulted in non-significant differences between both periods ($Z = -1.177$; $p > 0.05$; $n = 12$). The average monthly *THgF* values of both periods peaked in September and October (3.5 and 3.4 μg m^{-2}, respectively), while the lowest values occurred in January and February with averages < 0.2 μg m^{-2}. Birch leaves were the litterfall fraction that contributed the most to the annual *THgF* (73 %), being mainly concentrated from midspring to autumn (Fig. 2), with monthly fluxes peaking in September and October (≈ 3.0 μg m^{-2}; Fig. 3). The Hg deposition fluxes through birch leaves were significantly higher ($U = 3462.0$; $p < 0.01$; $n = 193$) in 2019–2020 (11.3 μg m^{-2} yr^{-1}) than in 2020–2021 (8.6 μg m^{-2} yr^{-1}) (Fig. 3). Miscellaneous constituted the second most relevant litterfall fraction, responsible for 13 % and 21 % of annual *THgF* to the forest floor in 2019–2020 and 2020–2021, respectively (Fig. 2). Therefore, the annual Hg deposition fluxes associated with miscellaneous were 1.9 μg m^{-2} yr^{-1} (2019–2020) and 2.5 μg m^{-2} yr^{-1} (2020 − 2021), with the highest mean

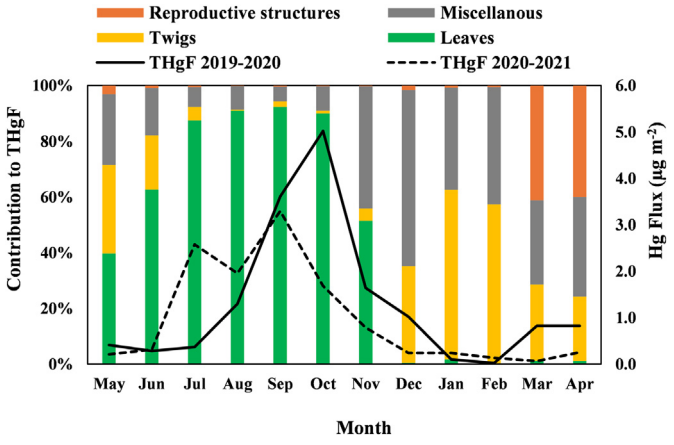

Fig. 2. Monthly variation of total Hg flux through litterfall (*THgF*) over the two studied periods (solid and dashed lines) and monthly contribution (%) of each litterfall fraction to *THgF* (bars).

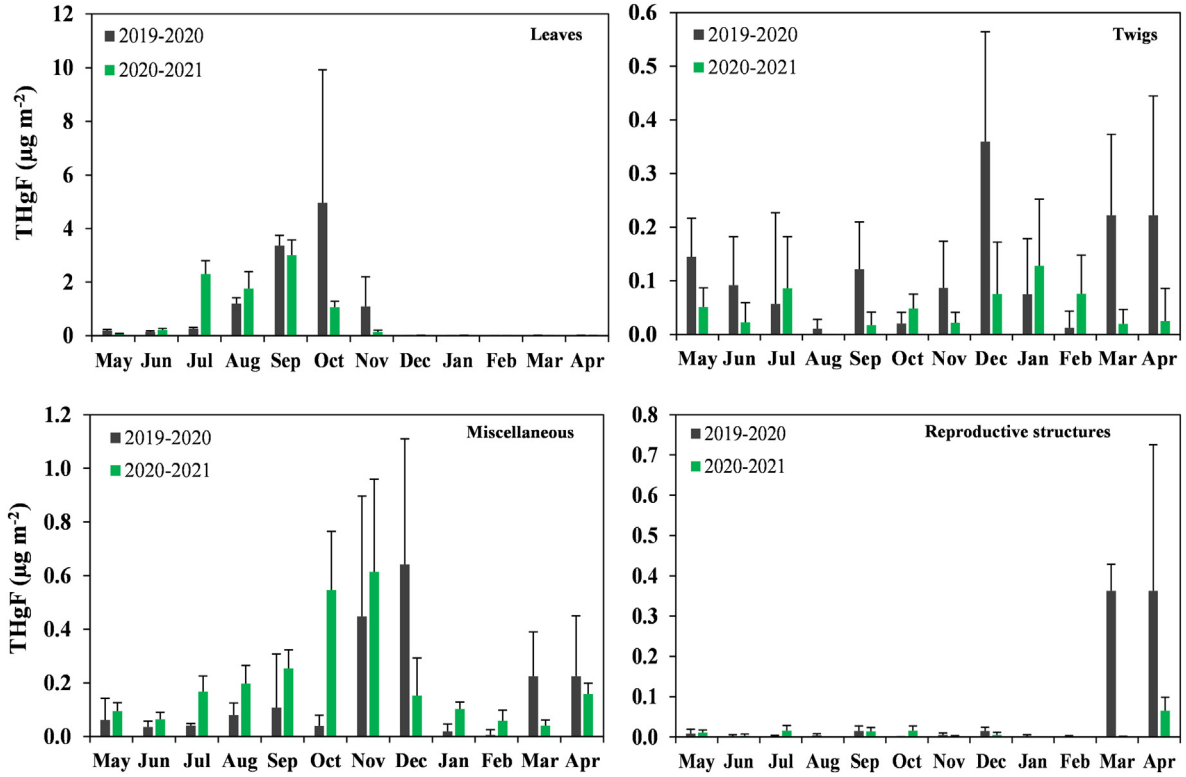

Fig. 3. Monthly average and standard deviation (error bars) of Hg deposition flux in leaves, twigs, miscellaneous and reproductive structures during the two periods studied.

monthly values registered in November (0.5 µg m^{-2}). The deposition fluxes of Hg through miscellaneous showed significant differences between the studied periods (U = 3943.0; p < 0.01; *n* = 227). The annual fluxes of Hg through the deposition of twigs were 1.4 and 0.6 µg m^{-2} yr^{-1}, whereas reproductive structures showed values of 0.78 and 0.13 µg m^{-2} yr^{-1} for 2019–2020 and 2020–2021, respectively (Fig. 3). The contribution of both fractions to the annual *THgF* was below 10 %, although reproductive structures have some relevance during March and April and twigs from December to May (Fig. 2).

3.4. Mercury concentration and storage in aboveground birch biomass

The mean concentrations of total Hg (*THg*) in different tissues of aboveground biomass of birch trees are shown in Table 2. Total Hg increased as the diameter of branches decreased in the sequence: thick branches (0.9 ± 0.1 µg kg^{-1}) < fine branches (1.7 ± 1.5 µg kg^{-1}) < twigs (24.7 ± 5.2 µg kg^{-1}). Low mean values of *THg* were found in bole wood (1.8 ± 0.4 µg kg^{-1}), comparable to those observed in fine branches, as well as in newly sprouted leaves (3.7 ± 0.7 µg kg^{-1}). Intermediate *THg* mean values were found in bark samples (11.7 ± 1.3 µg kg^{-1}). Values of *THg* varied significantly among the different plant tissues (H = 32.671; $p < 0.01$; *n* = 38).

The total amount of Hg accumulated in the whole aboveground biomass (*THgW*) was 532.0 mg ha^{-1}, being bole wood, bark and twigs the tissues that contributed the most to *THgW* (87 %), with 144.6, 158.6 and 159.9 mg ha^{-1}, respectively (Table 2). On the other hand, thick and fine branches and newly sprouted leaves stored 24.0, 25.2 and 19.6 mg Hg ha^{-1}, respectively (Table 2), values that were one order of magnitude lower than in bole wood, bark and twigs.

3.5. Mercury concentration and pools in the soil profile

Soils collected in the birch stand are characterized by an acid pH in the organic horizons. Soil acidity diminished considerably with depth in the mineral soil, i.e. from 3.9 at 0–5 cm layer to 4.9 at 50–60 cm (Table 3). Total organic C and N are high in the O layers (> 391 and > 15 g kg^{-1}, respectively), steadily decreasing until reaching the lowest values at 50–60 cm (33 and 2 g kg^{-1} of C and N, respectively). The C/N ratio varied scarcely in the mineral soil (range 12–15) and the sum of exchangeable base cations (Ca, Mg, K and Na) was <1 $cmol_c$ kg^{-1} in most of the mineral soil. A more detailed description of the physico-chemical soil properties can be found elsewhere (Table S4).

Regarding the levels of *THg* in the studied soil profiles, the mean concentration showed in the Oe + Oa layer (124 ± 13 µg kg^{-1}) was higher than in the Oi subhorizon (46 ± 7 µg kg^{-1}) (Fig. 4). In the mineral soil, *THg* ranged from 24 to 136 µg kg^{-1}, with the highest values occurring in the uppermost centimetres of the mineral soil (0–5 cm). On the other hand, *THg* decreased with mineral soil depth up to the 15–20 (33 µg kg^{-1}) and 20–30 cm (24 µg kg^{-1}) layers depending on the soil profile,

Table 2
Average and standard deviation of total Hg concentration (*THg*), biomass (*W*) and total Hg in biomass (*THgW*) of each aboveground plant tissue in each subplot.

Plant tissue	Subplot	THg	W	THgW
		µg kg^{-1}	Mg ha^{-1}	mg ha^{-1}
Newly sprouted leaves	1	4.1 ± 1.1	5.4 ± 0.0	22.0 ± 6.1
	2	3.4 ± 0.1	6.3 ± 0.0	21.8 ± 0.8
	3	3.5 ± 0.3	4.4 ± 0.0	15.2 ± 1.4
Twigs	1	21.4 ± 5.2	6.5 ± 0.0	139.8 ± 33.8
	2	24.1 ± 4.8	7.5 ± 0.0	181.8 ± 35.9
	3	28.5 ± 4.4	5.5 ± 0.0	158.1 ± 24.4
Fine branches	1	1.3 ± 0.3	14.3 ± 0.0	17.9 ± 4.9
	2	2.6 ± 2.6	17.3 ± 0.0	45.1 ± 44.9
	3	1.1 ± 0.3	11.4 ± 0.0	12.6 ± 3.0
Thick branches	1	0.9 ± 0.1	26.2 ± 0.0	23.6 ± 3.4
	2	1.0 ± 0.0	1.0 ± 0.0	30.9 ± 3.8
	3	0.9 ± 0.1	0.9 ± 0.0	21.7 ± 2.7
Bole wood	1	1.6 ± 0.0	83.3 ± 0.0	135.6 ± 1.2
	2	1.5 ± 0.1	99.3 ± 0.0	150.2 ± 1.9
	3	2.3 ± 0.2	64.6 ± 0.0	148.1 ± 2.1
Bark	1	12.3 ± 0.0	13.4 ± 0.0	164.1 ± 0.4
	2	12.4 ± 0.1	16.5 ± 0.0	203.8 ± 0.5
	3	9.8 ± 0.1	10.5 ± 0.0	102.5 ± 0.4

Table 3
Mean values and standard deviation (±) of some physico-chemical soil properties.

Soil layer	BD[a]	pHw	C	N	C/N	SB[a]
	g cm^{-3}		g kg^{-1}	g kg^{-1}		cmol$_c$ kg^{-1}
Oi	0.04 ± 0.01	4.3 ± 0.4	481 ± 11	15.0 ± 0.4	32 ± 1	28.2 ± 1.3
Oe + Oa	0.15 ± 0.02	4.2 ± 0.5	391 ± 50	18.3 ± 1.5	21 ± 1	11.9 ± 2.7
0–5	0.47 ± 0.01	3.9 ± 0.1	174 ± 32	12.1 ± 3.5	15 ± 2	1.9 ± 0.1
5–10	0.79 ± 0.00	4.3 ± 0.3	104 ± 15	8.0 ± 2.1	13 ± 2	0.9 ± 0.4
10–15	0.70 ± 0.10	4.5 ± 0.3	80 ± 22	6.4 ± 1.8	13 ± 0	0.6 ± 0.3
15–20	0.87 ± 0.09	4.7 ± 0.1	60 ± 8	5.1 ± 1.1	12 ± 1	0.5 ± 0.3
20–30	0.83 ± 0.03	4.7 ± 0.1	51 ± 9	4.0 ± 0.2	13 ± 2	0.6 ± 0.2
30–40	1.01 ± 0.15	4.8 ± 0.0	41 ± 2	3.0 ± 0.4	14 ± 1	0.6 ± 0.0
40–50	0.89 ± 0.12	4.8 ± 0.0	44 ± 8	2.9 ± 0.6	15 ± 0	0.8 ± 0.2
50–60	0.95 ± 0.04	4.9 ± 0.0	33 ± 14	2.2 ± 0.8	15 ± 0	0.6 ± 0.1

[a] BD and SB are the bulk density and the sum of exchangeable base cations, respectively.

rising again in the deeper soil layers until reaching values close to 90–100 μg kg^{-1}. The parental material on which the birch plot is located presents a *THg* value of 14.7 μg kg^{-1}. The average soil Hg pool (*PHg*) in the Oe + Oa layers was 1.0 ± 0.2 mg m^{-2} (Fig. 4), being two orders of magnitude higher than in the Oi subhorizon (0.02 ± 0.00 mg m^{-2}). The values of *PHg* in the mineral soil ranged from 1.1 to 9.5 mg m^{-2}, with the highest *THg* storage occurring in the deeper soil layers (below 30–40 or 40–50 cm, Fig. 4). Values of *PHg* in the whole mineral soil were 32 and 42 mg m^{-2} for profiles 1 and 2, being much higher than the Hg stored in the organic horizons where *PHg* ranged from 0.7 to 1.2 mg m^{-2}.

4. Discussion

4.1. Litterfall fluxes

The annual total litterfall flux (*TLF*) obtained in the present study was 2–5 times higher than the fluxes reported for silver birch (*Betula pendula*) in northern (Hansson et al., 2011) and central Europe (Carnol and Bazgir, 2013; Jagodziński et al., 2018), which varied between 120 and 285 g m^{-2} yr^{-1}. Latitudinal differences would be a factor explaining the greater litterfall fluxes found in the present study (at southern Europe) compared to other European locations. In this regard, Matala et al. (2008) found a strong relationship between litterfall fluxes and latitude, whereas Wang et al. (2016) also reported that litterfall fluxes diminished from low latitudes (tropic and subtropic biomes) to high latitudes (boreal biomes).

Leaves as the main fraction of *TLF* in the studied birch forest (Table S1) were consistent with what is expected in forests dominated by deciduous species (Hansen et al., 2009; Neumann et al., 2018), although their contribution (78 %) was somewhat higher than values in the range 56–67 % reported in mixed deciduous forests (that included birch species) from Belgium (Staelens et al., 2011; Carnol and Bazgir, 2013). The period during which the highest birch leaf fall occurred was somewhat longer (July–October) than that reported by Staelens et al. (2011), who found that 90 % of birch leaves fell from August to October. Even an additional month, as in our case, could influence the turnover of wilted leaves in the upper soil layers with consequences on Hg dynamics. The contribution of twigs and reproductive structures to annual *TLF* was lower than that reported in the abovementioned studies, where the ranges of twigs and reproductive structures inputs were 22–23 % and 10–21 %, respectively (Staelens et al., 2011; Carnol and Bazgir, 2013). The random temporal pattern of twigs flux could be partly explained by the occurrence of storms (accompanied by high rainfall and winds) and frosts, as monthly twig fluxes showed a correlation with accumulated precipitation ($\rho = 0.246$; $p < 0.01$; $n = 219$) and mean minimum temperatures ($\rho = -0.244$; $p < 0.01$; $n = 219$). In this regard, the wind proved to be a relevant factor for twig damage and subsequent fall in deciduous and coniferous forests (Díaz-Maroto and Vila-Lameiro, 2006;

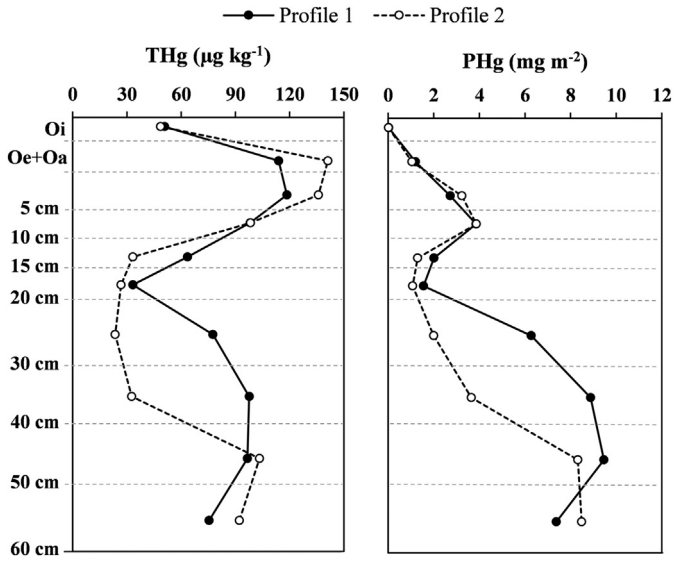

Fig. 4. Total Hg concentration (*THg*) and Hg pool (*PHg*) in the organic and mineral layers of the two soil profiles studied.

Portillo-Estrada et al., 2013). The peak of reproductive structures in litterfall samples in March–April (Table S1) was due to the shedding of male and female catkins that mainly occurs at this time (Jato et al., 2007). Regarding miscellaneous, the highest fluxes were found during periods characterized by the fall of moss/lichen pieces as well as biomass remains (leaves/needles, acorns, seeds, etc.) from tree species other than birch.

4.2. Mercury concentration in litterfall fractions

The statistically significant variations found for *THg* among the different litterfall fractions were probably the result of the joint effect of factors such as the presence/absence of stomata (Laacouri et al., 2013), metabolic processes and vegetation activity (Jiskra et al., 2018) and the length of the air exposure period (Bushey et al., 2008). In general, leaves (or needles) are widely recognized as the most active plant tissue involved in Hg accumulation (Yang et al., 2018; Zhou et al., 2017, 2021), which justifies that birch leaves constitute the litterfall fraction with the highest *THg* values (Table S2), excluding the miscellaneous which do not represent the birch biomass. The gradual increase of *THg* observed in birch leaves during the growing season (from March to September; Fig. 1) is not limited to deciduous species (Rea et al., 2002; Bushey et al., 2008; Gómez-Armesto et al., 2020b), but was also observed in multi-year coniferous needles (Hutnik et al., 2014; Lyapina, 2018; Navrátil et al., 2019; Wohlgemuth et al., 2020; Méndez-López et al., 2022b). The increase in *THg* content in birch leaves throughout spring and summer is attributed to the intensification of physiological activity (photosynthesis), with the subsequent increase in gas exchange through stomata and the passive uptake of atmospheric Hg (Laacouri et al., 2013).

The estimated Hg accumulation rate in birch leaves for the present study (0.18 $\mu g\ kg^{-1}\ day^{-1}$; Fig. 1) is within the range of values reported in North America for species of the genus *Betula* (0.12 to 0.22 $\mu g\ kg^{-1}\ day^{-1}$) (Bushey et al., 2008; Blackwell and Driscoll, 2015; Olson et al., 2019). Our estimate of the rate of Hg accumulation in birch leaves cannot be compared to others from European birch forests as, to the best of our knowledge, this parameter has not been determined so far in birch forests. However, the Hg accumulation rate we estimated for birch leaves was in the range of values (0.09–0.35 $\mu g\ kg^{-1}\ day^{-1}$) reported for deciduous species worldwide (Bushey et al., 2008; Blackwell et al., 2014; Fu et al., 2016; Gómez-Armesto et al., 2020b). The gradual increase of *THg* in birch foliage did not finish with the end of the growing season and the decline of leaf physiological activity, but continued as long as leaves remained exposed to the atmosphere on the tree branches, as evidenced by the higher *THg* values observed in birch leaves collected in January (Table S2). We have considered some possible explanations for this circumstance. First, the retention of atmospheric Hg by tree leaves can continue by non-stomatal mechanisms (Stamenkovic and Gustin, 2009), and second, the increase in *THg* concentrations could be due to the loss of mass of weak foliar tissues while Hg remains bound to the remaining and more durable tissues (Poissant et al., 2008). In addition, the observed increase in THg in leaves collected in January could also be attributed to PBM deposited on the leaf surface as a consequence of changes in environmental conditions (cold and less precipitation) at the end of the season, which may favour the mobilisation of dust particles from the soil surface.

Considering the same growing periods, values of *THg* in birch leaves obtained in the present study were slightly higher than those reported in forests from temperate and boreal areas of Europe and North America (Rea et al., 2002; Hall and St. Louis, 2004; Bushey et al., 2008; Larssen et al., 2008; Blackwell and Driscoll, 2015; Richardson and Friedland, 2015; Pleijel et al., 2021). In contrast, in Asian temperate forests, Zhou et al. (2017) found higher *THg* values (averages between 51 and 54 $\mu g\ kg^{-1}$) in leaves of species of the genus *Betula* than in the present study. The distinctive behavior of *Betula* species may explain these differences in foliar *THg*, but local and regional climatic characteristics (precipitation, temperature, wind) affecting tree physiology should also be taken into account as key factors in the variation of *THg* in birch leaves (Yang et al., 2019; Wohlgemuth et al., 2022). Moreover, in the case of Chinese studies, the influence of local Hg emission sources on high *THg* contents cannot be ruled out.

The annual average of *THg* in twigs during the two studied periods was similar to the mean value (15–19 $\mu g\ kg^{-1}$) reported for birch in northern Europe (Larssen et al., 2008). On the contrary, samples of birch twigs in temperate Asian forests showed lower mean *THg* within the range 7–8 $\mu g\ kg^{-1}$ (Zhou et al., 2017). The differences found for *THg* in twigs could be related to their exposure time and position in the canopy, a fact that has been previously observed in leaves (Bushey et al., 2008; Siwik et al., 2009; Wohlgemuth et al., 2020). No further reasons can be provided because it was not possible to obtain information on the position in the canopy and age of the twigs collected in the litterfall collectors.

Total Hg values found in reproductive structures (catkins) were the lowest compared to other litterfall fractions (Table S2), probably because their growth period is very short (March and April). On the contrary, miscellaneous showed the highest mean *THg* values, probably due to the presence of moss and lichen remains, which have been proved to accumulate larger amounts of Hg (Zhou et al., 2021). Moreover, the diversity in the type and origin of the plant tissues composing the miscellaneous fraction would explain the variation observed in the monthly *THg* values (Table S2). Most studies worldwide do not consider reproductive structures and miscellaneous in the assessment of Hg accumulation and deposition through litterfall to forest soils, which could lead to an underestimation of Hg deposition in forest ecosystems. This finding is in line with that recently evidenced by Zhou et al. (2021), who highlight the importance of some tissues (lichens, mosses, bark, etc.) as additional contributors to Hg deposition in forests, which are traditionally not considered in individual fractions in studies focused on Hg deposition through litterfall.

4.3. Mercury deposition fluxes through litterfall

The annual total Hg deposition fluxes through litterfall (*THgF*) obtained in the two periods studied (15.4 and 11.7 $\mu g\ m^{-2}\ yr^{-1}$) were higher than the range reported by St. Louis et al. (2019) in a birch wood from boreal forests in Canada (6.2–9.4 $\mu g\ m^{-2}\ yr^{-1}$). Although comparisons with other studies should be made with caution because of the distinctive composition of tree species and their influence on annual *THgF* (Hansson et al., 2011; Juillerat et al., 2012; Richardson and Friedland, 2015; Wang et al., 2016), our values were higher than those reported in mixed deciduous forests containing birch species in the U.S., which ranged from 3.6 to 9.3 $\mu g\ m^{-2}\ yr^{-1}$ (Demers et al., 2007; Graydon et al., 2008; Blackwell and Driscoll, 2015; Risch et al., 2017). However, comparable values of annual *THgF* (10.0–15.3 $\mu g\ m^{-2}\ yr^{-1}$) were obtained in other deciduous forests of the U.S. (Blackwell and Driscoll, 2015; Risch et al., 2017) as well as from temperate Asian deciduous forest (12.9 $\mu g\ m^{-2}\ yr^{-1}$; Zhou et al., 2017). On the contrary, Richardson and Friedland (2015) obtained an annual *THgF* twice as high as ours (mean 24 $\mu g\ m^{-2}\ yr^{-1}$).

The lack of significant differences in monthly *THgF* among the two studied periods agrees with previous research carried out close to the study area in which Hg deposition through litterfall was assessed in a forest dominated by another deciduous species (*Quercus robur*) (Gómez-Armesto et al., 2020b). This suggests that more years of monitoring are needed for a suitable assessment of the interannual variability of Hg deposition through litterfall.

The highest Hg fluxes observed from summer to early autumn (July–November), which accounted for 77.5 and 87.7 % of the annual *THgF* in 2019–2020 and 2020–2021 (Fig. 2), respectively, coincide with the period when almost all (> 90 %) birch foliage falls and leaves show high Hg levels (Table S2). Annual *THgF* levels are determined mostly by the flux of leaves in the litterfall than by their *THg* concentration, which is supported by the close correlation ($\rho = 0.986$; $p < 0.01$; $n = 193$) found between the total annual Hg flux through litterfall and the total annual litterfall flux. This assertion has already been reported in previous studies (Wang et al., 2016; Risch et al., 2017; Gómez-Armesto et al., 2020b). The strong connection between annual *THgF* and annual *TLF* would explain why Hg deposition

fluxes through birch leaves were higher in 2019–2020 than in 2020–2021 (Fig. 3), as the annual leaf flux was higher in the first period (2019–2020) (Table S1).

The relevance of miscellaneous as the second most important litterfall fraction contributing to annual *THgF* was consistent with the high ability of the plant tissues included in this fraction to capture atmospheric Hg. Moreover, miscellaneous not only showed the highest mean annual values of *THg* among the assessed litterfall fractions (Table S2) but also contributed largely to the total litterfall flux, especially in the 2020–2021 period (Fig. S1). On the other hand, the low contribution of twigs to annual *THgF* (Fig. 2) could be explained by their low *THg* concentrations because of the limited Hg uptake by woody tissues (Assad et al., 2016). However, not accounting for Hg inputs through woody tissues could lead to an underestimation of total Hg deposition through vegetation, as reported Wang et al. (2020). In the case of reproductive structures, their short period of exposure to air would prevent them from participating significantly in the capture of atmospheric Hg and its subsequent transfer to the soil surface through litterfall. However, the peak in the flux of catkins observed in December 2019 (7.4 g m^{-2}, Table S1), which occurred after a long period of strong winds and abundant rainfall in the study area, and the relatively high values of *THg* in reproductive structures during December 2020 (Table S2), could have contributed exceptionally to the *THgF* more than expected.

4.4. Mercury concentration and storage in aboveground birch biomass

The total concentration of Hg in newly sprouted birch leaves was considerably lower than the values (10–54 μg kg^{-1}) reported for birch foliage in other studies (Zhou et al., 2017; Yang et al., 2018). Such differences are likely associated with the extremely short exposure time to air masses of the leaves analyzed in the present study, being only two to three weeks. Differences in *THg* in birch leaves with respect to the abovementioned studies would be notably reduced if compared to the *THg* concentrations we observed in well-developed birch leaves (i.e. those collected during the mid-growing season, in July), when they reach *THg* levels of 20–24 μg kg^{-1}. Values of *THg* in birch bole wood were low, but of the same order as previous studies (Zhou et al., 2017; Yang et al., 2018; Yanai et al., 2020). The low overall *THg* content in bole wood reflects limitations for Hg translocation to aboveground plant tissues from the root system (Cui et al., 2014; Assad et al., 2016). In that regard, recent findings suggested that Hg in bole wood could be translocated from foliage, rather than from bark and roots (Arnold et al., 2018; Navrátil et al., 2018; Peckham et al., 2019; Yanai et al., 2020). Regarding bark samples, the *THg* values registered were similar to those obtained by Zhou et al. (2017) (12.3–13.4 μg kg^{-1}), but somewhat greater than those reported by Yang et al. (2018), which ranged from 3.2 to 7.5 μg kg^{-1}. The higher *THg* values in bark than in bole wood are probably the result of a higher ability of the former to adsorb Hg due to its particular chemical composition (Viso et al., 2021) as well as its more direct exposure to air masses (Chiarantini et al., 2016). This could also explain why twigs (Ø < 0.5 cm) were the plant tissue with the highest *THg* since, due to their scarce thickness, it was not possible to separate the thin bark from the woody tissue. In general, the *THg* values found in bole wood and bark were in the same order than those reported by Zhou and Obrist (2021) in deciduous broadleaf forests worldwide with mean levels of 2 and 9 μg kg^{-1}, respectively.

The total Hg pool in the aboveground biomass (Fig. 5), as the sum of Hg stored in bole wood, bark, branches, twigs and leaves, was higher than the value reported for mixed broadleaf forests containing birch species in Asia (335 mg ha^{-1}; Zhou et al., 2017). Despite the differences, we agree with Zhou et al. (2017) on the role of woody tissues (bole wood, bark and twigs) as the main compartment in which Hg is stored, who found a value (83 %) quite close to that obtained in the present study (87 %). The total Hg pool in the aboveground biomass obtained in the present study was of the same order of magnitude than the values reported by other authors (200 and 330 mg ha^{-1}) in different deciduous forests (Obrist et al., 2012; Richardson and Friedland, 2015). Therefore, although woody tissues are not directly involved in the uptake of atmospheric Hg (GEM), they represent an important reservoir of Hg that should be taken into account for a more reliable estimation of Hg pools in forest ecosystems.

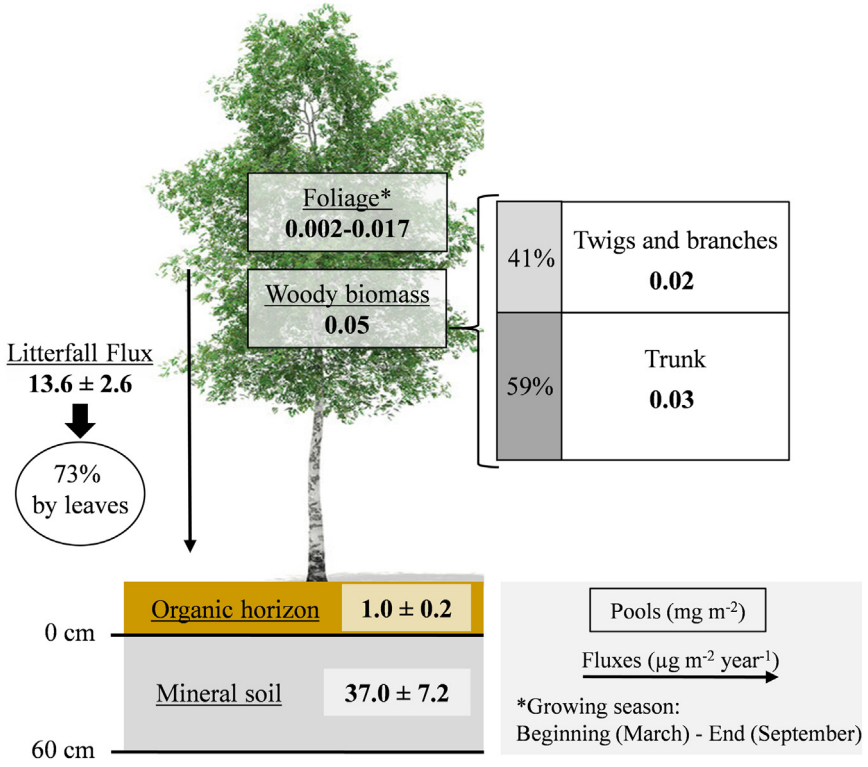

Fig. 5. Total Hg pools (mg m^{-2}) in aboveground biomass and soil profile and Hg deposition flux by litterfall (μg m^{-2} $year^{-1}$) in the study plot.

The pool of Hg stored in tree foliage was very dependent on the development stage of leaves, as *THg* in leaves increased over the growing season (Fig. 1). Thus, the estimated Hg pool in the biomass of birch leaves at the end of the growing season (170.8 mg ha^{-1} in September) is almost 9 times higher than the value obtained in newly sprouted leaves at the beginning of the growing season (19.6 mg ha^{-1} in March). In addition, it should be noted that the foliar Hg pool is highly dynamic compared to other aboveground plant tissues, so that only two growing seasons are necessary for leaf biomass to reach the Hg levels stored in woody tissues (bole wood and bark). Furthermore, all Hg stored in birch foliage will be transferred annually to the soil surface through litterfall, which once again highlights the key role of tree foliage in the sequestration of atmospheric Hg, affecting its fate in the plant-soil interactions taking place in forest ecosystems.

4.5. Mercury concentration and pools in soils

The *THg* values obtained in the Oi and Oe + Oa horizons were in the range of values reported by Gruba et al. (2019) for the entire organic horizon of forests dominated by birch species in central Europe (average *THg* 60 μg kg^{-1}). However, higher *THg* values were found in organic horizons under mixed deciduous forests containing birch species in North America, ranging from 148 to 395 μg kg^{-1} (Demers et al., 2007; Blackwell et al., 2014; Blackwell and Driscoll, 2015; Richardson and Friedland, 2015).

The values of *THg* in the Oi subhorizons were slightly lower than in the birch leaves collected from the litterfall samplers. This fact can be justified by Hg loss after leaves fall through processes such as leaching, run-off or re-emission to the atmosphere (Beckers and Rinklebe, 2017). Moreover, the Oi layers are also composed of other plant debris constituting a substantial mass fraction of this organic subhorizon but with considerably lower *THg*. On the other hand, the significant increase in *THg* from the Oi (fresh undecomposed biomass) to the Oe + Oa subhorizon (old decomposed biomass) can be related to a faster loss of C than Hg during litter decomposition as was indicated by Pokharel and Obrist (2011), which favours the accumulation of Hg in the more humified organic layer. In the present study, the influence of litter decomposition on *THg* levels in the organic horizons is supported by the correlation between C/N ratio (an estimate of the degree of organic matter decomposition) and *THg* ($\rho = -0.786$; $p < 0.05$; $n = 8$). A similar relationship between *THg* and C/N ratio in organic horizons was reported in previous studies (Obrist et al., 2011; Navrátil et al., 2014, 2016). Similar to our results, higher *THg* concentrations in the most decomposed organic subhorizons are commonly found in forest soils worldwide (Obrist et al., 2011; Navrátil et al., 2014; Zhou et al., 2017; Gómez-Armesto et al., 2020b; Méndez-López et al., 2022a).

The *THg* concentrations found in the mineral soil are within the range of values reported in non-polluted areas worldwide (Blackwell et al., 2014; Richardson and Friedland, 2015; Zhou et al., 2017; Gómez-Armesto et al., 2020a,b). The trend of decreasing *THg* with soil depth in the mineral soil is often related to a progressive decline of organic C towards deeper soil layers (Richardson et al., 2013; Zhou et al., 2013; Peña-Rodríguez et al., 2014; Navrátil et al., 2014, 2016). However, the pattern of *THg* distribution with soil depth in the mineral soil does not coincide with that shown by organic C and N. In fact, there were no significant correlations between *THg* and total organic C and N, suggesting that other soil compounds rather than organic matter may be involved in the distribution of Hg in the mineral soil, such as Al and Fe oxyhydroxides (Gabriel and Williamson, 2004; Richardson et al., 2013; Navrátil et al., 2016; Gómez-Armesto et al., 2020a, 2021).

The values of total Hg pool (*PHg*) found in the studied soils, considering organic and mineral layers (33 and 43 mg m^{-2}), were 4 to 6 times higher than those obtained in a birch-dominated forest in Central Europe (Gruba et al., 2019) and mixed deciduous forests from Asia (Zhou et al., 2017) and north-eastern USA (Richardson and Friedland, 2015). However, similar Hg pools were reported in a hardwood plot partly dominated by yellow birch in North America (41 mg m^{-2}, Blackwell et al., 2014) and in a deciduous forest in central Europe (45 mg m^{-2}, Navrátil et al., 2016).

The higher *PHg* in the mineral soil, compared to the organic horizons, was expected given their greater bulk density and thickness (Fig. 5). In addition to physical and morphological properties, soil chemical properties also contributed notably to the greater Hg storage in the mineral soil. Thus, in contrast to what occurred with *THg*, *PHg* correlated negatively with total C ($\rho = -0.524$; $p < 0.05$; $n = 16$) and N ($\rho = -0.597$; $p < 0.05$; $n = 16$) and positively with the C/N ratio ($\rho = 0.721$; $p < 0.05$; $n = 16$). These relationships lead to an increase in Hg storage in the deeper mineral soil layers (Fig. 4), despite showing the lower values of total organic C and total N. However, the positive relationship of *THg* with the C/N ratio suggests that this scarce amount of organic matter is quite active in the retention of Hg in the mineral soil. On the other hand, as was abovementioned, previous studies indicated that Hg storage in the mineral soil is also highly dependent on the presence of Fe and Al compounds (Richardson et al., 2013; Gómez-Armesto et al., 2020a,b). In this sense, *PHg* was positively correlated with Al compounds such as the estimated organic matter complexes of Al (Al_p; $\rho = 0.588$; $p < 0.05$; $n = 16$) or the total content of crystalline and non-crystalline Al compounds (Al_n; $\rho = 0.579$; $p < 0.05$; $n = 16$), which could explain the vertical pattern of *PHg* found through the mineral soil layers. In addition, although *THg* in soil parent material was relatively low (14.7 μg kg^{-1}), it could also contribute to *PHg* in deeper layers of the mineral soil. The largest accumulation of Hg in the mineral soil, accounting for up to 97 % of the Hg stored in the whole profile, was consistent with that reported in previous studies, where the mineral soil layers accumulated between 86 and 99 % of the total Hg pool (Navrátil et al., 2016; Gruba et al., 2019; Gómez-Armesto et al., 2020b).

5. Conclusions

The litterfall flux and the deposition flux of Hg varied significantly among the studied litterfall fractions. Birch leaves were the major contributor to the total Hg deposition flux by litterfall, being more conditioned by the flux of leaf biomass than by their Hg concentration. Under the current global warming scenario, in which the period of leaf biomass activity is likely to be extended, there would be an increase in the levels of Hg assimilated by leaves and, therefore, a greater deposition of Hg to the forest floor.

The results obtained for Hg pools in the aboveground biomass revealed that, although not actively involved in the uptake of atmospheric Hg, woody tissues (bole wood, bark, branches and twigs) represent the largest Hg reservoir. On the other hand, the pool of Hg in birch leaves varied with their growth stage, as the Hg concentration increases over the growing season. However, it should be noted that the Hg stored in birch leaves will be annually transferred to soil surface through litterfall, highlighting the key role of tree foliage in the fate of Hg in forest ecosystems.

Once deposited in the soil, Hg tends to accumulate in the organic horizon and in the uppermost layers of the mineral horizon, which is strongly linked to the decomposition process of organic matter. However, the uppermost soil layers of forest ecosystems are more exposed to alterations due to climate change, land use changes and forest management, so that their role as a sink for Hg may be affected. On the contrary, the deeper layers of the mineral horizon are exempt from being altered by environmental changes, and the presence of some soil components, such as Fe and Al compounds, could favour the retention and accumulation of Hg in them. Therefore, future studies should pay more attention to the role of deeper soil layers (below 40 cm) in the biogeochemical cycling of Hg, because of their potential ability to immobilize Hg and reduce the possibility of reaching groundwater.

Data availability

Data will be made available on request.

Declaration of competing interest

The authors declare that they have no known competing financial interests or personal relationships that could have appeared to influence the work reported in this paper.

Acknowledgments

M. Méndez-López acknowledges the predoctoral grant FPU of Ministerio de Educación y Formación Profesional (FPU17/05484). We are grateful to Alexandre Cendón González, representative of the Comunidad de Montes de Santiago de Covelo, for making the study plot available to us. We also greatly appreciate the valuable collaboration of Mario López Fernández during the fieldwork. It is also recognized the financial support of the Consellería de Cultura, Educación e Universidade (Xunta de Galicia) through the contract ED431C2021/46-GRC granted to the research group BV1 of the University of Vigo and the research project ED431F2018/06-EXCELENCIA.

Appendix A. Supplementary data

Supplementary data to this article can be found online at https://doi.org/10.1016/j.scitotenv.2022.158937.

References

Agnan, Y., Le Dantec, T., Moore, C.W., Edwards, G.C., Obrist, D., 2016. New constraints on terrestrial surface-atmosphere fluxes of gaseous elemental mercury using a global database. Environ. Sci. Technol. 50, 507–524. https://doi.org/10.1021/acs.est.5b04013.

Arnold, J., Gustin, M.S., Weisberg, P.J., 2018. Evidence for nonstomatal uptake of hg by Aspen and translocation of hg from foliage to tree rings in austrian pine. Environ. Sci. Technol. 52, 1174–1182. https://doi.org/10.1021/acs.est.7b04468.

Assad, M., Parelle, J., Cazaux, D., Gimbert, F., Chalot, M., Tatin-Froux, F., 2016. Mercury uptake into poplar leaves. Chemosphere 146, 1–7. https://doi.org/10.1016/j.chemosphere.2015.11.103.

Ballabio, C., Jiskra, M., Osterwalder, S., Borrelli, P., Montanarella, L., Panagos, P., 2021. A spatial assessment of mercury content in the European Union topsoil. Sci. Total Environ. 769. https://doi.org/10.1016/j.scitotenv.2020.144755.

Beck, P., Caudullo, G., De Rigo, D., Tinner, W., 2016. Betula pendula, Betula pubescens and other birches in Europe: distribution, habitat, usage and threats. Eur. Atlas For. Tree Species 70–73.

Beckers, F., Rinklebe, J., 2017. Cycling of mercury in the environment: sources, fate, and human health implications: a review. Crit. Rev. Environ. Sci. Technol. 47 (9), 693–794. https://doi.org/10.1080/10643389.2017.1326277.

Blackwell, B.D., Driscoll, C.T., 2015. Deposition of mercury in forests along a montane elevation gradient. Environ. Sci. Technol. 49, 5363–5370. https://doi.org/10.1021/es505928w.

Blackwell, B.D., Driscoll, C.T., Maxwell, J.A., Holsen, T.M., 2014. Changing climate alters inputs and pathways of mercury deposition to forested ecosystems. Biogeochemistry 119, 215–228. https://doi.org/10.1007/s10533-014-9961-6.

Bushey, J.T., Nallana, A.G., Montesdeoca, M.R., Driscoll, C.T., 2008. Mercury dynamics of a northern hardwood canopy. Atmos. Environ. 42, 6905–6914. https://doi.org/10.1016/j.atmosenv.2008.05.043.

Carnol, M., Bazgir, M., 2013. Nutrient return to the forest floor through litter and throughfall under 7 forest species after conversion from Norway spruce. For. Ecol. Manag. 309, 66–75. https://doi.org/10.1016/j.foreco.2013.04.008.

Chiarantini, L., Rimondi, V., Benvenuti, M., Beutel, M.W., Costagliola, P., Gonnelli, C., Lattanzi, P., Paolieri, M., 2016. Black pine (Pinus nigra) barks as biomonitors of airborne mercury pollution. Sci. Total Environ. 569–570, 105–113. https://doi.org/10.1016/j.scitotenv.2016.06.029.

Cui, L., Feng, X., Lin, C.-J., Wang, X., Meng, B., Wang, X., Wang, H., 2014. Accumulation and translocation of 198Hg in four crop species. Environ. Toxicol. Chem. 33, 334–340. https://doi.org/10.1002/etc.2443.

Demers, J.D., Driscoll, C.T., Fahey, T.J., Yavitt, J.B., 2007. Mercury cycling in litter and soil in different forest types in the Adirondack region, New York, USA. Ecol. Appl. 17, 1341–1351. https://doi.org/10.1890/06-1697.1.

Díaz-Maroto, I.J., Vila-Lameiro, P., 2006. Litter production and composition in natural stands of Quercus robur L. (Galicia, Spain). Pol. J. Ecol. 54 (3), 429–439.

Driscoll, C.T., Mason, R.P., Chan, H.M., Jacob, D.J., Pirrone, N., 2013. Mercury as a global pollutant: sources, pathways, and effects. Environ. Sci. Technol. 47, 4967–4983. https://doi.org/10.1021/es305071v.

EUFORGEN Secretariat. (s. f.). Betula pendula - EUFORGEN European forest genetic resources programme. Last access date: 04/07/2022 https://www.euforgen.org/species/betula-pendula/.

Friedli, H.R., Radke, L.F., Payne, N.J., McRae, D.J., Lynham, T.J., Blake, T.W., 2007. Mercury in vegetation and organic soil at an upland boreal forest site in Prince Albert National Park, Saskatchewan, Canada. J. Geophys. Res. Biogeosci. 112, G01004. https://doi.org/10.1029/2005JG000061.

Fu, X., Yang, X., Lang, X., Zhou, J., Zhang, H., Yu, B., Yan, H., Lin, C.-J., Feng, X., 2016. Atmospheric wet and litterfall mercury deposition at urban and rural sites in China. Atmos. Chem. Phys. 16, 11547–11562. https://doi.org/10.5194/acp-16-11547-2016.

Gabriel, M.C., Williamson, D.G., 2004. Principal biogeochemical factors affecting the speciation and transport of mercury through the terrestrial environment. Environ. Geochem. Health 26, 421–434. https://doi.org/10.1007/s10653-004-1308-0.

Gómez-Armesto, A., Martínez-Cortizas, A., Ferro-Vázquez, C., Méndez-López, M., Arias-Estévez, M., Nóvoa-Muñoz, J.C., 2020a. Modelling hg mobility in podzols: role of soil components and environmental implications. Environ. Pollut. 260. https://doi.org/10.1016/j.envpol.2020.114040.

Gómez-Armesto, A., Méndez-López, M., Pérez-Rodríguez, P., Fernández-Calviño, D., Arias-Estévez, M., Nóvoa-Muñoz, J.C., 2020b. Litterfall hg deposition to an oak forest soil from southwestern Europe. J. Environ. Manag. 269, 110858.

Gómez-Armesto, A., Méndez-López, M., Marques, P., Pontevedra-Pombal, X., Monteiro, F., Madeira, M., Arias-Estévez, M., Nóvoa-Muñoz, J.C., 2021. Patterning total mercury distribution in coastal podzolic soils from an Atlantic area: influence of pedogenetic processes and soil components. Catena 206. https://doi.org/10.1016/j.catena.2021.105540.

Gómez-García, E., Crecente-Campo, F., Diéguez-Aranda, U., 2013. Above-ground biomass equations for birch (Betula pubescens ehrh.) and pedunculate oak (Quercus robur L.) in north western Spain | tarifas de biomasa aérea Para abedul (Betula pubescens ehrh.) y roble (Quercus robur L.) en el noroeste de España. Madera Bosques 19, 71–91.

Graydon, J.A., St. Louis, V.L., Hintelmann, H., Lindberg, S.E., Sandilands, K.A., Rudd, J.W.M., Kelly, C.A., Hall, B.D., Mowat, L.D., 2008. Long-term wet and dry deposition of total and methyl mercury in the remote boreal ecoregion of Canada. Environ. Sci. Technol. 42, 8345–8351.

Grigal, D.F., 2003. Mercury sequestration in forests and peatlands: a review. J. Environ. Qual. 32, 393–405.

Gruba, P., Socha, J., Pietrzykowski, M., Pasychnyk, D., 2019. Tree species affects the concentration of total mercury (Hg) in forest soils: evidence from a forest soil inventory in Poland. Sci. Total Environ. 647, 141–148. https://doi.org/10.1016/j.scitotenv.2018.07.452.

Hall, B.D., St. Louis, V.L., 2004. Methylmercury and total mercury in plant litter decomposing in upland forests and flooded landscapes. Environ. Sci. Technol. 38, 5010–5021. https://doi.org/10.1021/es049800q.

Hansen, K., Vesterdal, L., Schmidt, I.K., Gundersen, P., Sevel, L., Bastrup-Birk, A., Pedersen, L.B., Bille-Hansen, J., 2009. Litterfall and nutrient return in five tree species in a common garden experiment. For. Ecol. Manag. https://doi.org/10.1016/j.foreco.2009.02.021.

Hansson, K., Olsson, B.A., Olsson, M., Johansson, U., Kleja, D.B., 2011. Differences in soil properties in adjacent stands of scots pine, Norway spruce and silver birch in SW Sweden. For. Ecol. Manag. 262, 522–530. https://doi.org/10.1016/j.foreco.2011.04.021.

Hutnik, R.J., McClenahen, J.R., Long, R.P., Davis, D.D., 2014. Mercury accumulation in Pinus nigra (Austrian Pine). Northeast. Nat. 21, 529–540.

IUSS Working Group WRB, 2015. World Reference Base for Soil Resources 2014, Update 2015. International Soil Classification System for Naming Soils and Creating Legends for Soil Maps. World Soil Resources Reports, p. 106.

Jagodziński, A.M., Wierzcholska, S., Dyderski, M.K., Horodecki, P., Rusińska, A., Gdula, A.K., Kasprowicz, M., 2018. Tree species effects on bryophyte guilds on a reclaimed post-mining site. Ecol. Eng. 110, 117–127. https://doi.org/10.1016/j.ecoleng.2017.10.015.

Jato, V., Rodríguez-Rajo, F.J., Aira, M.J., 2007. Use of phenological and pollen-production data for interpreting atmospheric birch pollen curves. Ann. Agric. Environ. Med. 14, 271–280.

Jiskra, M., Wiederhold, J.G., Skyllberg, U., Kronberg, R.-M., Hajdas, I., Kretzschmar, R., 2015. Mercury deposition and re-emission pathways in boreal forest soils investigated with hg isotope signatures. Environ. Sci. Technol. 49, 7188–7196.

Jiskra, M., Sonke, J.E., Obrist, D., Bieser, J., Ebinghaus, R., Myhre, C.L., Pfaffhuber, K.A., Wängberg, I., Kyllönen, K., Worthy, D., Martin, L.G., Labuschagne, C., Mkololo, T., Ramonet, M., Magand, O., Dommergue, A., 2018. A vegetation control on seasonal variations in global atmospheric mercury concentrations. Nat. Geosci. 11, 244–250. https://doi.org/10.1038/s41561-018-0078-8.

Juillerat, J.I., Ross, D.S., Bank, M.S., 2012. Mercury in litterfall and upper soil horizons in forested ecosystems in Vermont, USA. Environ. Toxicol. Chem. 31, 1720–1729. https://doi.org/10.1002/etc.1896.

Laacouri, A., Nater, E.A., Kolka, R.K., 2013. Distribution and uptake dynamics of mercury in leaves of common deciduous tree species in Minnesota, U.S.A. Environ. Sci. Technol. https://doi.org/10.1021/es401357z.

Larssen, T., de Wit, H.A., Wiker, M., Halse, K., 2008. Mercury budget of a small forested boreal catchment in Southeast Norway. Sci. Total Environ. 404, 290–296. https://doi.org/10.1016/j.scitotenv.2008.03.013.

Lyapina, E.E., 2018. Dynamics and features of mercury accumulation in coniferous trees of Tomsk region. IOP Conference Series: Earth and Environmental Science, p. 12051.

Ma, M., Wang, D., Du, H., Sun, T., Zhao, Z., Wei, S., 2015. Atmospheric mercury deposition and its contribution of the regional atmospheric transport to mercury pollution at a national forest nature reserve, Southwest China. Environ. Sci. Pollut. Res. 22, 20007–20018. https://doi.org/10.1007/s11356-015-5152-9.

Martínez Cortizas, A., Pérez Alberti, A., 1999. Atlas climático de Galicia. Santiago de Compostela, Spain: Consellería de Medioambiente, Xunta de Galicia, p. 207.

Matala, J., Kellomäki, S., Nuutinen, T., 2008. Litterfall in relation to volume growth of trees: analysis based on literature. Scand. J. For. Res. https://doi.org/10.1080/02827580802036176.

Méndez-López, M., Gómez-Armesto, A., Alonso-Vega, F., Pontevedra-Pombal, X., Fonseca, F., de Figueiredo, T., Arias-Estévez, M., Nóvoa-Muñoz, J.C., 2022a. The role of afforestation species as a driver of hg accumulation in organic horizons of forest soils from a Mediterranean mountain area in SW Europe. Sci. Total Environ. 827. https://doi.org/10.1016/j.scitotenv.2022.154345.

Méndez-López, M., Gómez-Armesto, A., Eimil-Fraga, C., Alonso-Vega, F., Rodríguez-Soalleiro, R., Álvarez-Rodríguez, E., Arias-Estévez, M., Nóvoa-Muñoz, J.C., 2022b. Needle age and precipitation as drivers of hg accumulation and deposition in coniferous forests from a southwestern European Atlantic region. Environ. Res., 114223 https://doi.org/10.1016/j.envres.2022.114223.

Munthe, J., Hultberg, H., Iverfeldt, Å., 1995. Mechanisms of deposition of methylmercury and mercury to coniferous forests. Water Air Soil Pollut. 80, 363–371. https://doi.org/10.1007/BF01189686.

Munthe, J., Bishop, K., Driscoll, C., Graydon, J., Hultberg, H., Lindberg, S.E., Matzer, E., Porvari, P., Rea, A., Schwesig, D., 2004. Input-output of hg in forested catchments in Europe and North America. Mater. Geoenviron. 51, 1243–1246.

Navrátil, T., Shanley, J., Rohovec, J., Hojdová, M., Penížek, V., Buchtová, J., 2014. Distribution and pools of mercury in czech forest soils. Water Air Soil Pollut. 225. https://doi.org/10.1007/s11270-013-1829-1.

Navrátil, T., Shanley, J.B., Rohovec, J., Oulehle, F., Šimecek, M., Houška, J., Cudlín, P., 2016. Soil mercury distribution in adjacent coniferous and deciduous stands highly impacted by acid rain in the Ore Mountains, Czech Republic. Appl. Geochem. 75, 63–75. https://doi.org/10.1016/j.apgeochem.2016.10.005.

Navrátil, T., Nováková, T., Shanley, J.B., Rohovec, J., Matoušková, Š., Vaňková, M., Norton, S.A., 2018. Larch tree rings as a tool for reconstructing 20th century central european atmospheric mercury trends. Environ. Sci. Technol. 52, 11060–11068. https://doi.org/10.1021/acs.est.8b02117.

Navrátil, T., Nováková, T., Roll, M., Shanley, J.B., Kopáček, J., Rohovec, J., Kaňa, J., Cudlín, P., 2019. Decreasing litterfall mercury deposition in central european coniferous forests and effects of bark beetle infestation. Sci. Total Environ. https://doi.org/10.1016/j.scitotenv.2019.05.093.

Neumann, M., Ukonmaanaho, L., Johnson, J., Benham, S., Vesterdal, L., Novotný, R., Verstraeten, A., Lundin, L., Thimonier, A., Michopoulos, P., Hasenauer, H., 2018. Quantifying carbon and nutrient input from litterfall in european forests using field observations and modeling. Glob. Biogeochem. Cycles 32, 784–798. https://doi.org/10.1029/2017GB005825.

Obrist, D., Johnson, D.W., Lindberg, S.E., Luo, Y., Hararuk, O., Bracho, R., Battles, J.J., Dail, D.B., Edmonds, R.L., Monson, R.K., Ollinger, S.V., Pallardy, S.G., Pregitzer, K.S., Todd, D.E., 2011. Mercury distribution across 14 U.S. Forests. Part I: spatial patterns of concentrations in biomass, litter, and soils. Environ. Sci. Technol. 45, 3974–3981. https://doi.org/10.1021/es104384m.

Obrist, D., Johnson, D.W., Edmonds, R.L., 2012. Effects of vegetation type on mercury concentrations and pools in two adjacent coniferous and deciduous forests. J. Plant Nutr. Soil Sci. 175, 68–77. https://doi.org/10.1002/jpln.201000415.

Obrist, D., Kirk, J.L., Zhang, L., Sunderland, E.M., Jiskra, M., Selin, N.E., 2018. A review of global environmental mercury processes in response to human and natural perturbations: changes of emissions, climate, and land use. Ambio 47, 116–140. https://doi.org/10.1007/s13280-017-1004-9.

Obrist, D., Roy, E.M., Harrison, J.L., Kwong, C.F., William Munger, J., Moosmüller, H., Romero, C.D., Sun, S., Zhou, J., Commane, R., 2021. Previously unaccounted atmospheric mercury deposition in a midlatitude deciduous forest. Proc. Natl. Acad. Sci. U. S. A. 118. https://doi.org/10.1073/pnas.2105477118.

Olson, C.L., Jiskra, M., Sonke, J.E., Obrist, D., 2019. Mercury in tundra vegetation of Alaska: spatial and temporal dynamics and stable isotope patterns. Sci. Total Environ. 660, 1502–1512. https://doi.org/10.1016/j.scitotenv.2019.01.058.

Peckham, M.A., Gustin, M.S., Weisberg, P.J., Weiss-Penzias, P., 2019. Results of a controlled field experiment to assess the use of tree tissue concentrations as bioindicators of air hg. Biogeochemistry 142, 265–279. https://doi.org/10.1007/s10533-018-0533-z.

Peña-Rodríguez, S., Pontevedra-Pombal, X., Gayoso, E.G.R., Moretto, A., Mansilla, R., Cutillas-Barreiro, L., Arias-Estévez, M., Nóvoa-Muñoz, J.C., 2014. Mercury distribution in a toposequence of sub-Antarctic forest soils of Tierra del Fuego (Argentina) as consequence of the prevailing soil processes. Geoderma 232–234, 130–140. https://doi.org/10.1016/j.geoderma.2014.04.040.

Pleijel, H., Klingberg, J., Nerentorp, M., Broberg, M.C., Nyirambangutse, B., Munthe, J., Wallin, G., 2021. Mercury accumulation in leaves of different plant types-the significance of tissue age and specific leaf area. Biogeosciences 18, 6313–6328. https://doi.org/10.5194/bg-18-6313-2021.

Poissant, L., Pilote, M., Yumvihoze, E., Lean, D., 2008. Mercury concentrations and foliage/atmosphere fluxes in a maple forest ecosystem in Québec, Canada. J. Geophys. Res. Atmos. https://doi.org/10.1029/2007JD009510.

Pokharel, A.K., Obrist, D., 2011. Fate of mercury in tree litter during decomposition. Biogeosciences 8, 2507–2521. https://doi.org/10.5194/bg-8-2507-2011.

Portillo-Estrada, M., Korhonen, J.F.J., Pihlatie, M., Pumpanen, J., Frumau, A.K.F., Morillas, L., Tosens, T., Niinemets, U., 2013. Inter- and intra-annual variations in canopy fine litterfall and carbon and nitrogen inputs to the forest floor in two European coniferous forests. Ann. For. Sci. 70, 367–379. https://doi.org/10.1007/s13595-013-0273-0.

Rea, A.W., Lindberg, S.E., Keeler, G.J., 2001. Dry deposition and foliar leaching of mercury and selected trace elements in deciduous forest throughfall. Atmos. Environ. 35, 3453–3462. https://doi.org/10.1016/S1352-2310(01)00133-9.

Rea, A.W., Lindberg, S.E., Scherbatskoy, T., Keeler, G.J., 2002. Mercury accumulation in foliage over time in two northern mixed-hardwood forests. Water Air Soil Pollut. 133, 49–67. https://doi.org/10.1023/A:1012919731598.

Richardson, J.B., Friedland, A.J., 2015. Mercury in coniferous and deciduous upland forests in northern New England, USA: implications of climate change. Biogeosciences 12, 6737–6749. https://doi.org/10.5194/bg-12-6737-2015.

Richardson, J.B., Friedland, A.J., Engerbretson, T.R., Kaste, J.M., Jackson, B.P., 2013. Spatial and vertical distribution of mercury in upland forest soils across the northeastern United States. Environ. Pollut. 182, 127–134. https://doi.org/10.1016/j.envpol.2013.07.011.

Risch, M.R., DeWild, J.F., Gay, D.A., Zhang, L., Boyer, E.W., Krabbenhoft, D.P., 2017. Atmospheric mercury deposition to forests in the eastern USA. Environ. Pollut. 228, 8–18. https://doi.org/10.1016/j.envpol.2017.05.004.

Rutter, A.P., Schauer, J.J., Shafer, M.M., Creswell, J.E., Olson, M.R., Robinson, M., Collins, R.M., Parman, A.M., Katzman, T.L., Mallek, J.L., 2011. Dry deposition of gaseous elemental mercury to plants and soils using mercury stable isotopes in a controlled environment. Atmos. Environ. https://doi.org/10.1016/j.atmosenv.2010.11.025.

Siwik, E.I.H., Campbell, L.M., Mierle, G., 2009. Fine-scale mercury trends in temperate deciduous tree leaves from Ontario, Canada. Sci. Total Environ. 407, 6275–6279. https://doi.org/10.1016/j.scitotenv.2009.08.044.

St. Louis, V.L., Graydon, J.A., Lehnherr, I., Amos, H.M., Sunderland, E.M., St. Pierre, K.A., Emmerton, C.A., Sandilands, K., Tate, M., Steffen, A., Humphreys, E.R., 2019. Atmospheric concentrations and wet/dry loadings of mercury at the remote experimental lakes area, northwestern ontario, Canada. Environ. Sci. Technol. https://doi.org/10.1021/acs.est.9b01338.

Staelens, J., Nachtergale, L., De Schrijver, A., Vanhellemont, M., Wuyts, K., Verheyen, K., 2011. Spatio-temporal litterfall dynamics in a 60-year-old mixed deciduous forest. Ann. For. Sci. https://doi.org/10.1007/s13595-011-0010-5.

Stamenkovic, J., Gustin, M.S., 2009. Nonstomatal versus stomatal uptake of atmospheric mercury. Environ. Sci. Technol. 43, 1367–1372. https://doi.org/10.1021/es801583a.

Sun, X., Liu, F., Zhang, Q., Li, Y., Zhang, L., Wang, J., Zhang, H., Wang, C., Wang, X., 2021. Biotic and climatic controls on the interannual variation in canopy litterfall of a deciduous broad-leaved forest. Agric. For. Meteorol. 307. https://doi.org/10.1016/j.agrformet.2021.108483.

Viso, S., Rivera, S., Martinez-Coronado, A., Esbrí, J.M., Moreno, M.M., Higueras, P., 2021. Biomonitoring of hg0, hg2+ and particulate hg in a mining context using tree barks. Int. J. Environ. Res. Public Health 18. https://doi.org/10.3390/ijerph18105191.

Wang, X., Bao, Z., Lin, C.-J., Yuan, W., Feng, X., 2016. Assessment of global mercury deposition through litterfall. Environ. Sci. Technol. 50, 8548–8557. https://doi.org/10.1021/acs.est.5b06351.

Wang, X., Yuan, W., Lu, Z., Lin, C.-J., Yin, R., Li, F., Feng, X., 2019. Effects of precipitation on mercury accumulation on subtropical montane Forest floor: implications on climate forcing. J. Geophys. Res. Biogeosci. https://doi.org/10.1029/2018JG004809.

Wang, X., Yuan, W., Lin, C.-J., Luo, J., Wang, F., Feng, X., Fu, X., Liu, C., 2020. Underestimated sink of atmospheric mercury in a deglaciated Forest chronosequence. Environ. Sci. Technol. 54, 8083–8093. https://doi.org/10.1021/acs.est.0c01667.

Wohlgemuth, L., Osterwalder, S., Joseph, C., Kahmen, A., Hoch, G., Alewell, C., Jiskra, M., 2020. A bottom-up quantification of foliar mercury uptake fluxes across Europe. Biogeosciences 17, 6441–6456. https://doi.org/10.5194/bg-17-6441-2020.

Wohlgemuth, L., Rautio, P., Ahrends, B., Russ, A., Vesterdal, L., Waldner, P., Timmermann, V., Eickenscheidt, N., Fürst, A., Greve, M., Roskams, P., Thimonier, A., Nicolas, M., Kowalska, A., Ingerslev, M., Merilä, P., Benham, S., Iacoban, C., Hoch, G., Alewell, C., Jiskra, M., 2022. Physiological and climate controls on foliar mercury uptake by european tree species. Biogeosciences 19 (5), 1335–1353. https://doi.org/10.5194/bg-19-1335-2022.

Wright, L.P., Zhang, L., Marsik, F.J., 2016. Overview of mercury dry deposition, litterfall, and throughfall studies. Atmos. Chem. Phys. 16, 13399–13416. https://doi.org/10.5194/acp-16-13399-2016.

Wu, F., Jiang, Y., Wen, Y., Zhao, S., Xu, H., 2021. Spatial synchrony in the start and end of the thermal growing season has different trends in the mid-high latitudes of the northern hemisphere. Environ. Res. Lett. 16. https://doi.org/10.1088/1748-9326/ac3696.

Yanai, R.D., Yang, Y., Wild, A.D., Smith, K.T., Driscoll, C.T., 2020. New approaches to understand mercury in trees: radial and longitudinal patterns of mercury in tree rings and genetic control of mercury in maple sap. Water Air Soil Pollut. 231. https://doi.org/10.1007/s11270-020-04601-2.

Yang, Y., Yanai, R.D., Driscoll, C.T., Montesdeoca, M., Smith, K.T., 2018. Concentrations and content of mercury in bark, wood, and leaves in hardwoods and conifers in four forested sites in the northeastern USA. PLoS One 13. https://doi.org/10.1371/journal.pone.0196293.

Yang, Y., Meng, L., Yanai, R.D., Montesdeoca, M., Templer, P.H., Asbjornsen, H., Rustad, L.E., Driscoll, C.T., 2019. Climate change may alter mercury fluxes in northern hardwood forests. Biogeochemistry 146 (1), 1–16. https://doi.org/10.1007/s10533-019-00605-1.

Zhou, J., Obrist, D., 2021. Global mercury assimilation by vegetation. Environ. Sci. Technol. 55, 14245–14257. https://doi.org/10.1021/acs.est.1c03530.

Zhou, J., Feng, X., Liu, H., Zhang, H., Fu, X., Bao, Z., Wang, X., Zhang, Y., 2013. Examination of total mercury inputs by precipitation and litterfall in a remote upland forest of southwestern China. Atmos. Environ. 81, 364–372. https://doi.org/10.1016/j.atmosenv.2013.09.010.

Zhou, J., Wang, Z., Zhang, X., Gao, Y., 2017. Mercury concentrations and pools in four adjacent coniferous and deciduous upland forests in Beijing, China. J. Geophys. Res. Biogeosci. 122, 1260–1274. https://doi.org/10.1002/2017JG003776.

Zhou, J., Obrist, D., Dastoor, A., Jiskra, M., Ryjkov, A., 2021. Vegetation uptake of mercury and impacts on global cycling. Nat. Rev. Earth Environ. 2, 269–284. https://doi.org/10.1038/s43017-021-00146-y.

Zhu, W., Lin, C.-J., Wang, X., Sommar, J., Fu, X., Feng, X., 2016. Global observations and modeling of atmosphere-surface exchange of elemental mercury: a critical review. Atmos. Chem. Phys. 16, 4451–4480. https://doi.org/10.5194/acp-16-4451-2016.